Conformational Dependence of Carbon Monoxide Ligation Dynamics in Cytochrome c Oxidase†

Bih-Show Lou,‡ Randy W. Larsen,§,∥ Sunney I. Chan,§ and Mark R. Ondrias*,‡

Contribution from the Department of Chemistry, University of New Mexico, Albuquerque, New Mexico 87131, and Arthur Amos Noyes Laboratory of Chemical Physics,⊥ California Institute of Technology, Pasadena, California 91125. *Received January 27, 1992*

Abstract: Time-resolved optical studies have recently demonstrated that ligand photolysis and rebinding in fully reduced cytochrome *c* oxidase (Cco) is an extremely complicated process involving structural dynamics of both the proximal and distal heme pockets of cytochrome a_3. We have expanded upon these studies by examining the corresponding ligation dynamics in mixed-valence (MV) Cco, which is known to exist in a conformation that is structurally and kinetically distinct from fully reduced (FR) Cco. We report here time-resolved Raman results showing that while the promximal heme pocket dynamics of MV-Cco are similar to those of FR-Cco, the ligation dynamics of the distal pocket are affected by the protein conformational state.

Introduction

Cytochrome *c* oxidase (Cco) is the terminal electron acceptor in the mitochondrial respiratory chain. This integral membrane protein contains at least 13 functional subunits and four redox-active metal centers (two heme A chromophores and two Cu ions) which catalyze the four-electron reduction of dioxygen using electrons derived from ferrocytochrome *c* (see ref 1 for a general review). The redox-active metal centers are functionally organized into two pairs. Dioxygen binding and reduction occurs at a site located in subunit I consisting of a coupled heme A (cytochrome a_3) and a Cu ion (Cu_B). The remaining heme A/Cu_A pair is located on the cytosolic side of the inner membrane and catalyzes the electron transfer from cytochrome *c* to the binuclear cluster. In addition, cytochrome *c* oxidase participates in energy transduction by coupling electron transfer to the active transport of protons across the inner mitochondrial membrane.

The elucidation of the mechanism of redox-linked proton translocation in cytochrome *c* oxidase is of fundamental importance in the study of biological energy transduction. It is widely believed that one of the low-potential metal centers is the site of redox linkage in the enzyme, partly on the basis of the fact that the transfer of electrons from the low-potential metal centers to the binuclear site represents the largest free energy change in the catalytic cycle.[2-4] Recently, Gelles et al.[4] have proposed a functional model for proton translocation involving a redox-linked ligand-exchange reaction at the low-potential Cu_A. These studies demonstrate the importance of gating the flow of electrons as well as protons into and out of the pump site. The requirement of electron and proton gating as well as the apparent selectivity in electron-transfer pathways (i.e., pumping vs nonpumping electron-transfer pathways) necessitates at least two distinct types of conformational transitions which may be allosterically linked to the binuclear cluster. It has long been known that the spectroscopic behavior of cytochrome a_3 is predicated, to some degree, upon the redox state of the low-potential metal centers. Reduction of the low-potential metal cofactors affects both the optical properties[5-7] and the ligand-binding kinetics[7-10] of the catalytic site. The present work focuses upon the effects of conformational changes associated with the reduction of the low-potential metal centers on the ligation dynamics of cytochrome a_3.

In this study, we have used time-resolved resonance Raman spectroscopy (RRS) to compare the structural dynamics at the cytochrome a_3 site immediately following CO photolysis from fully reduced (FR) and CO mixed-valence (MV) Cco. RRS has proven to be a powerful tool for characterizing both the equilibrium structures and functionality of the hemes in Cco (see ref 11 for an excellent review). The catalytic intermediates of Cco have been studied using both static[12] and flow-flash techniques.[13-16] Time-resolved RRS has also been used to examine the structural relaxation of cytochrome a_3 subsequent to CO photolysis.[17] Recently, Woodruff and co-workers[18-21] have found that the dynamics subsequent to CO photolysis in the FR enzyme are complicated by CO binding to Cu_B and the rapid binding (<10 ps) of a photolabile endogenous ligand to cytochrome a_3. Our data extend these studies by characterizing the heme pocket dynamics subsequent to CO photolysis in MV-Cco and contrasting them to those of the FR enzyme.

* Author to whom correspondence should be sent.
† Research supported in part by Grants GM33330 (to M.R.O.) and GM22432 (to S.I.C.) from the National Institute of General Medical Sciences, U.S. Public Health Service.
‡ University of New Mexico.
§ California Institute of Technology.
∥ Present address: Department of Chemistry, University of Hawaii.
⊥ Contribution No. 8558 from the A. A. Noyes Laboratory.

(1) Wikstrom, M.; Klaab, K.; Saraste, M. In *Cytochrome Oxidase: A synthesis*; Academic Press: New York, 1981.
(2) Wikstrom, M.; Krab, K. *Biochim. Biophys. Acta* **1979**, *549*, 177-222.
(3) Chan, S. I.; Li, P. M. *Biochemistry* **1990**, *29*, 1-12.
(4) Gelles, J.; Blair, D. F.; Chan, S. I. *Biochim. Biophys. Acta* **1987**, *853*, 205-236.
(5) Wikstrom, M. F.; Harmon, H. J.; Ingledew, W. J.; Chance, B. *FEBS Lett.* **1976**, *65*, 259-277.
(6) Yong, F. C.; King, T. E. *Biochem. Biophys. Res. Commun.* **1970**, *40*, 1445-1451.
(7) Jensen, P.; Wilson, M. T.; Aasa, R.; Malmstrom, B. G. *Biochem. J.* **1984**, *224*, 829-837.
(8) Scholes, C. P.; Malmstrom, B. G. *FEBS Lett.* **1986**, *198*, 125-129.
(9) Greenwood, C.; Wilson, M. T.; Brunori, M. *Biochem. J.* **1974**, *137*, 205-215.
(10) Jones, M. G.; Bickar, D.; Wilson, M. T.; Brunori, M.; Colosimo, A.; Sarti, P. *Biochem. J.* **1984**, *220*, 57-66.
(11) Babcock, G. T. In *Biological Applications of Raman Spectroscopy*; Spiro, T. G., Ed.; Wiley & Sons: New York, 1988; Vol. 3.
(12) Larsen, R. W.; Li, W.; Copeland, R. A.; Witt, S. N.; Lou, S.; Chan, S. I.; Ondrias, M. R. *Biochemistry* **1990**, *29*, 10135-10140.
(13) Han, S.; Ching, Y.; Rousseau, D. L. *Biochemistry* **1990**, *29*, 1380-1384.
(14) Han, S.; Ching, Y.; Rousseau, D. L. *Proc. Natl. Acad. Sci. U.S.A.* **1990**, *87*, 2491-2495.
(15) Varotsis, C.; Woodruff, W. H.; Babcock, G. T. *J. Biol. Chem.* **1990**, *19*, 11131-11136.
(16) Varotsis, C.; Woodruff, W. H.; Babcock, G. T. *J. Am. Chem. Soc.* **1989**, *111*, 6439-6440.
(17) Findsen, E. W.; Centeno, J.; Babcock, G. T.; Ondrias, M. R. *J. Am. Chem. Soc.* **1987**, *109*, 5367-5372.
(18) Woodruff, W. H.; Einarsdottir, O.; Dyer, R. B.; Bagley, K. A.; Palmer, G.; Atherton, S. J.; Goldbeck, R. A.; Dawes, T. D.; Kiliger, D. S. *Proc. Natl. Acad. Sci. U.S.A.* **1991**, *88*, 2588-2592.
(19) Dyer, R. B.; Peterson, K. A.; Stoutland, P. O.; Woodruff, W. H. *J. Am. Chem. Soc.* **1991**, *113*, 6276-6277.
(20) Dyer, R. B.; Einarsdottir, O.; Killough, P. M.; Lopez-Garriga, J.; Woodruff, W. H. *J. Am. Chem. Soc.* **1989**, *111*, 7656-7659.
(21) Dyer, R. B.; Lopez-Garriga, J.; Einarsdottir, O.; Woodruff, W. H. *J. Am. Chem. Soc.* **1989**, *111*, 8962-8963.

0002-7863/93/1515-403$04.00/0

Materials and Methods

Cytochrome *c* oxidase (Cco) was isolated from bovine heart mitochondria by following a modification of the method of Hartzell and Beinert.[22] The enzyme was solubilized in 50 mM HEPES, 0.5% Brij-35 at pH 7.4, and stored at 77 K until needed. Cco concentration was determined using $\Delta\epsilon_{605nm}$ = 24 mM^{-1} cm^{-1} in the reduced minus oxidized optical spectrum.[23]

The FR-Cco–CO derivative (120 μM) was prepared by degassing the enzyme with 5 or 6 cycles of vacuum/N_2 in an anaerobic optical cell followed by the addition of a minimal amount of solid sodium dithionite under positive N_2 pressure. Full reduction was determined by monitoring the Δ(absorbance) at 605 nm. The sample was then subjected to 3–5 cycles of vacuum/CO with a final CO pressure over the sample of 1 atm. Formation of the FR-Cco–CO derivative was monitored by observing the appearance of the Soret band at 430 nm (Soret maximum for CO-bound cytochrome a_3). The CO mixed-valence species was prepared by incubating the degassed resting enzyme (120 μM) with CO (1 atm) in the dark overnight at room temperature. Formation of the derivative was verified by the appearance of a Soret band at 428 nm.

The time-resolved Raman spectrometer consists of two nanosecond-pulsed lasers synchronized to specific time delays (see ref 24 for a complete description). The delay time between the pump pulse and probe pulse was set using a digital delay generator (Cal Avionics 113br). The pump laser consists of a Quanta Ray DLII dye laser (Coumerin 540A dye) pumped by the third harmonic of a Quanta Ray Nd:YAG DCR II laser. The pump laser energy was ~3 mJ/pulse at 540 nm. The probe laser consists of a Molectron UV-24 N_2 laser pumping a DL14 dye laser with Coumerin 440 dye producing pulses of ~300 μJ/pulse at 440 nm with a repetition rate of ~10 Hz. The flux of the probe beam at the sample was modulated using either focusing optics or neutral density filters (see Results and figure captions for details). In our experiments, the "low power" for time-resolved RR spectra was obtained using defocused cylindrical optics yielding fluxes of ~2 × 10^5 W/(cm^2·s). The lowest power was obtained using cylindrical optics with a 1.5-OD neutral density filter (~2 × 10^4 W/(cm^2·s)), and the highest power was obtained using focused spherical optics (~1 × 10^7 W/(cm^2·s)). Intermediate laser fluxes were obtained by focusing or defocusing the cylindrical optics and by adding neutral density filters to the optical train with focused cylindrical optics.

Results

Figure 1A depicts the extent of CO photodissociation in FR-Cco as observed in the ν_4 region of the spectrum (1330–1400 cm^{-1}). The position of ν_4 for the unliganded FR form of Cco is 1356 cm^{-1}, while the position of ν_4 for the CO-bound derivative is 1368 cm^{-1}, in accordance with well-established assignments of heme *a* vibrational modes (see ref 11). The corresponding dependence of the low-frequency spectrum upon incident laser flux is shown in Figure 1B. The spectra displayed here were obtained using a single train of ~10-ns laser pulses to both photodissociate the ligand and generate the resonance Raman spectrum. At high laser fluxes, virtually all of the CO is photodissociated, as evidenced by a single band at ~1356 cm^{-1} in the ν_4 region (Figure 1A, trace f). Under these conditions, a prominent ν_{Fe-His} band is observed at ~222 cm^{-1} (Figure 1B, trace f), in accordance with the generation of a five-coordinate, high-spin cytochrome a_3 with a nonequilibrium heme-axial ligand geometry, as reported earlier.[17] Photolysis with lower power pulses (Figure 1A, traces a–e) produces difference behavior. Even though appreciable CO photodissociation occurs, the intensity of the ν_{Fe-His} band remains very low. In view of the extreme photolability of heme a_3–CO, careful measurements were required to quantify this phenomenon. Base-line spectra of the fully photolyzed (Figure 1A, trace f) and CO-bound (Figure 1A, trace a) species were used to deconvolute spectra of the partially photolyzed species. The extent of photolysis was estimated by determining linear combinations of the basis spectra which bounded the ν_4 band observed at intermediate laser fluencies (see Figure 1 for details). The intensity of ν_{Fe-His} was determined from low-fequency spectra (panel B of Figure 1) obtained under exactly the same conditions as the corresponding ν_4 spectra. Ratioing

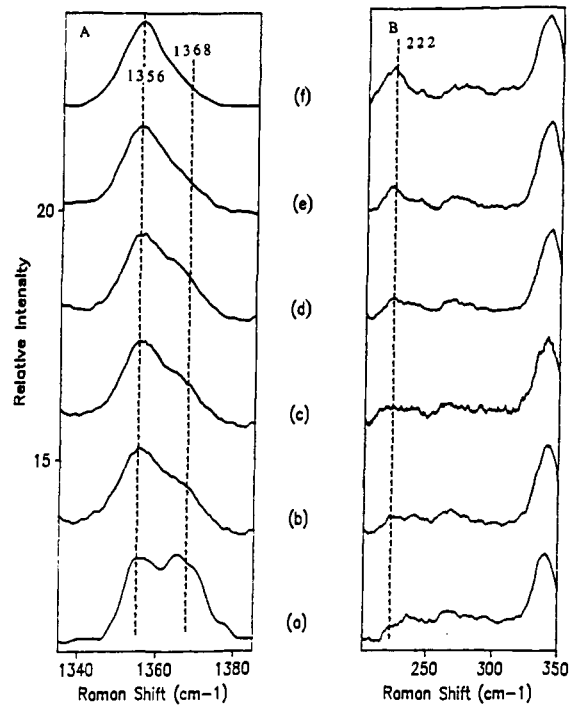

Figure 1. Power dependence of resonance Raman spectra of the CO-photolyzed fully reduced cytochrome *c* oxidase obtained using 10-ns pump–probe pulses (~350 μJ/pulse) in a single-pulse protocol. Panel A depicts the ν_4 region with (a) 1.5-OD neutral density filter with cylindrical optics (~2 × 10^4 W/(cm^2·s)), (b) a 0.7-OD neutral density filter with focused cylindrical optics (~1 × 10^5 W/(cm^2·s)), (c) defocused cylindrical optics (~3 × 10^5 W/(cm^2·s)), (d) a 0.3-OD neutral density filter with focused cylindrical optics (~4 × 10^5 W/(cm^2·s)), (e) focused cylindrical optics (~8 × 10^5 W/(cm^2·)), and (f) spherical optics (~1 × 10^7 W/(cm^2·s)). Panel B shows the low-frequency region obtained under identical conditions as panel A. Spectra are sums of 4–32 scans recorded at 15 cm^{-1}/min. Spectra a and f of panel A were smoothed with a 25-pt Squitsky–Golay protocol. The excitation wavelength was 440 nm, which preferentially enhances the modes of high-spin reduced heme a_3.

either the peak intensities of ν_{Fe-His} (221 cm^{-1}) and ν_8 (340 cm^{-1}) or their areas (obtained via protocols similar to that described in Figure 6) yielded, within experimental error, the same relationship between ν_{Fe-His} intensity and the extent of CO photolysis. This is depicted in Figure 2. Interestingly, the variations in the intensity of ν_{Fe-His} do not scale linearly with the extent of CO photodissociation, but depend only on the flux of the photolysis pulse. Woodruff and co-workers[18-21] have noted similar behavior using picosecond pulses.

The photodynamic behavior of the MV form of Cco following CO photodissociation is quite distinct from that of the FR enzyme. In Figure 3 we contrast the spectra of the 10-ns photolytic transients of the MV species with those of the FR-Cco (Figure 1) obtained under otherwise identical photolysis conditions. The ν_4 region (Figure 3A) of the MV enzyme is complicated by interference from ν_4 of the ferric cytochrome *a* (1372 cm^{-1}), which appears at a frequency similar to ν_4 for the CO-bound cytochrome a_3 (1368 cm^{-1}). Nevertheless, the extent of CO photodissociation can be gauged by the intensity of the peak at 1356 cm^{-1}. In contrast to the situation with FR-Cco, ν_{Fe-His} (Figure 3B) is prominent in the MV spectra at all laser fluxes. This difference is particularly evident under relatively mild laser powers (conditions under which spectra 3b and 3c were recorded), where ν_{Fe-His} is barely discernible in the case of FR-Cco. Both the resonance Raman spectra of the entire high-frequency region (1300–1700 cm^{-1}) (data not shown) and the optical absorption spectra obtained immediately after the RRS experiments confirmed that no significant photoreduction of cytochrome *a* had occurred in MV-Cco during acquisition of the Raman spectra.

Figure 4 depicts the temporal evolution of the five-coordinate, high-spin transient species of FR-Cco. CO was photodissociated with 540-nm pump pulses at high fluxes, and the time evolution

(22) Hartzell, C. R.; Beinert, H. *Biochim. Biophys. Acta* **1974**, *368*, 318–338.
(23) Ellis, W. R.; Wang, J. H.; Blair, D. F.; Gray, H. B.; Chan, S. I. *Biochemistry* **1986**, *25*, 161–167.
(24) Findsen, E. W. Ph.D. Dissertation, University of New Mexico, 1986.

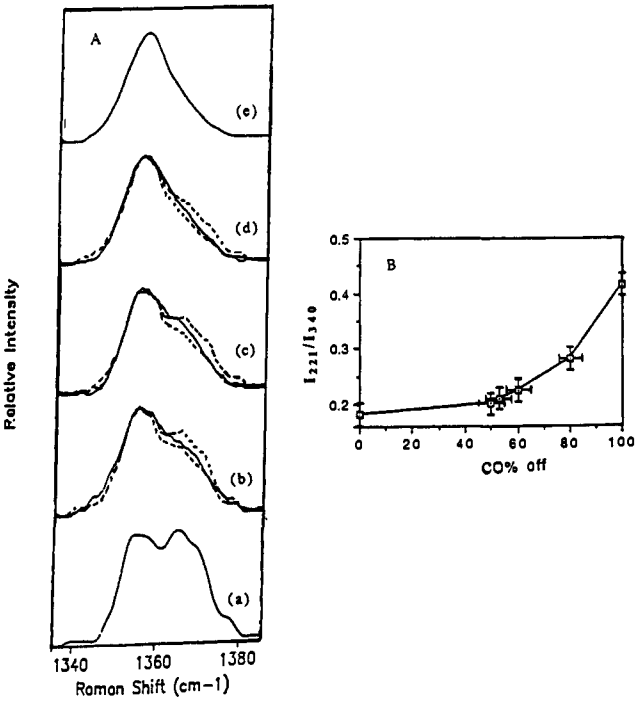

Figure 2. Quantification of the extent of CO photolysis and the intensity of ν_{Fe-His} as a function of laser flux. Panel A: CO photolysis. Spectra b–d show ν_4 as a function of laser flux (solid lines) bounded by linear combinations of fully photolyzed and unphotolyzed spectra (spectra e and a, respectively). Spectrum b is compared to 40/60 (lower dashed line) and 60/40 (upper dashed line) combinations of spectra e and a (e/a). Spectrum c is bounded by 50/50 and 70/30 ratios, while spectrum d is bracketed by linear combinations representing 70% and 90% photolysis (see text for details). Panel B: Comparison of ν_{Fe-His} intensity (measured at 222 cm^{-1}) vs extent of CO photolysis (see text for details).

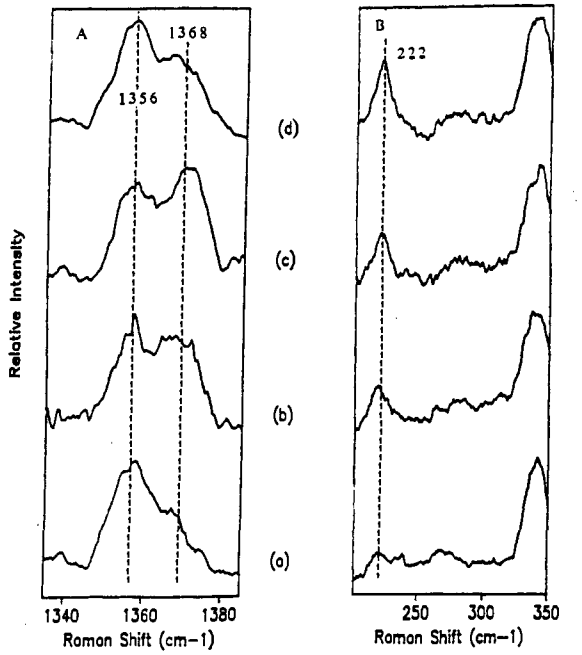

Figure 3. Power dependence of resonance Raman spectra of the CO-photolyzed mixed-valence cytochrome *c* oxidase obtained using the protocol described in Figure 1. Panel A depicts the ν_4 region. (a) Low-power (defocused cylindrical optics, $\sim 3 \times 10^5$ W/(cm^2·s)) spectrum of fully reduced CO complex. (b) Spectrum of CO mixed-valence complex at same flux as spectrum a. (c) MV CO spectrum using a 0.3-OD neutral density filter with focused cylindrical optics ($<2 \times 10^5$ W/(cm^2·s)). (d) MV CO spectrum using focused cylindrical optics ($>4 \times 10^5$ W/(cm^2·s)). Spectra are sums of 8–12 scans recorded at 15 cm^{-1}/min. Panel B shows the low-frequency region under the same conditions as in panel A.

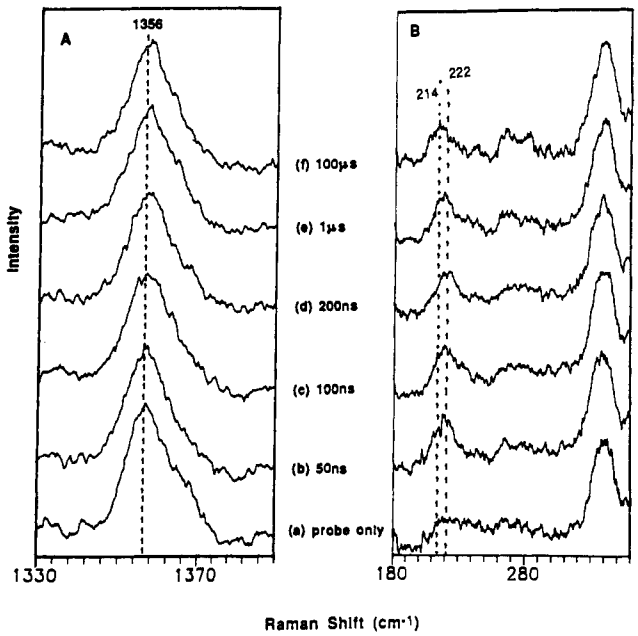

Figure 4. Time-resolved resonance Raman spectra of the FR cytochrome *c* oxidase subsequent to CO photolysis. A two-pulse protocol employed 540-nm pump pulses ($\sim 3 \times 10^6$ W/(cm^2·s)) and low-power 440-nm probe pulses ($\sim 3 \times 10^5$ W/(cm^2·s)). Panel A: ν_4 region. Panel B: Low-frequency region. Time delays between pump and probe pulses are given beside each spectrum. Spectra are sums of 4 scans.

of cytochrome a_3 was probed in the low-frequency region with low-flux 440-nm pulses following the initial intense photolysis pulses. Figure 4 clearly shows that the intense 540-nm pulses generate a five-coordinate, high-spin cytochrome a_3 in FR-Cco indistinguishable from that produced by pumping in the Soret band (ν_{Fe-His} = 222 cm^{-1}). The temporal behavior of ν_{Fe-His} of the FR species (ν_{Fe-His} = 222–214 cm^{-1}) was also, within experimental error, identical to that previously observed using higher power probe pulses ($\sim 1 \times 10^7$ W/(cm^2·s)).[17] Interestingly, there is *no* evidence that the "low-power" photolyzed cytochrome a_3 species observed in the FR enzyme is generated subsequent to the pump pulse.

The evolution of the cytochrome a_3 proximal pocket in photodissociated MV-Cco (Figure 5) is remarkably similar to that previously observed for the FR enzyme[17] and reproduced in this study (Figure 4). The data were further analyzed by curve-fitting the raw data following previously established methods (see ref 17). While quantification of the ν_{Fe-His} position is limited to ±1 cm^{-1}, the data are quite reproducible. It is clear that the Fe–His mode of cytochrome a_3 in both species evolves from $\sim$221 cm^{-1} to its equilibrium position at $\sim$215 cm^{-1} with $\tau_{1/2} \sim 10$ μs, following a $\sim$200-ns lag phase in which no relaxation takes place. Indeed, the data (see Figure 6 for details) suggest that ν_{Fe-His} may actually increase slightly in frequency during the first 100 ns subsequent to CO photodissociation. Neither the FR nor the MV species exhibits geminate ligand recombination on a sub-millisecond time scale. Both species, however, display relaxation of ν_{Fe-His} to its equilibrium position ($\sim$215 cm^{-1}) on a $\sim$10-μs time scale (Figure 6B). Thus, it is clear that the proximal heme pocket dynamics are not affected by differences between the MV and FR protein conformations.

Discussion

CO photodissociation from cytochrome a_3 is an extremely efficient process under a wide variety of conditions. It can be initiated by pumping either the B or Q bands of the heme even under low-temperature conditions.[25] Photodissociation of the CO-inhibited enzyme has long been used in both cryogenic and room temperature studies as a convenient means of initiating the catalytic cycle of Cco. The flow–flash protocol has been instru-

(25) Chance, B.; Saronico, C.; Leigh, J. S. *J. Biol. Chem.* **1975**, *250*, 9226–9237.

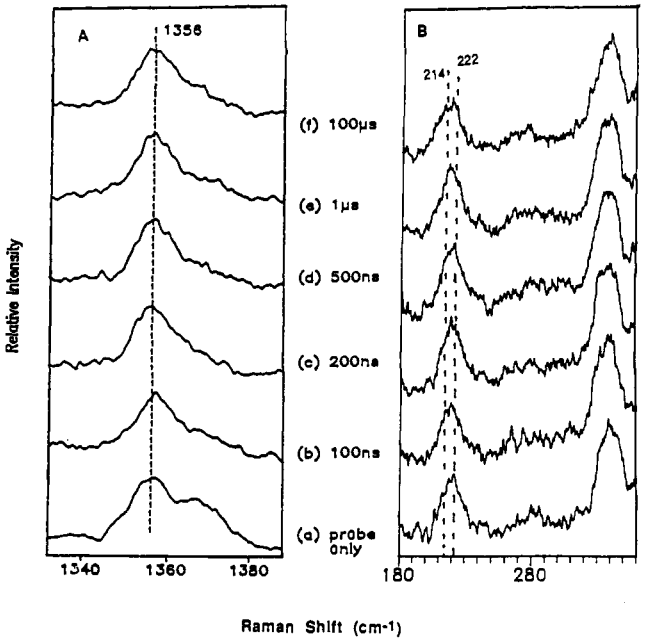

Figure 5. Time-resolved resonance Raman spectra of the MV enzyme subsequent to CO photolysis. The probe power at 440 nm is $\sim 4 \times 10^5$ W/(cm^2·s), and other conditions are the same as in Figure 4.

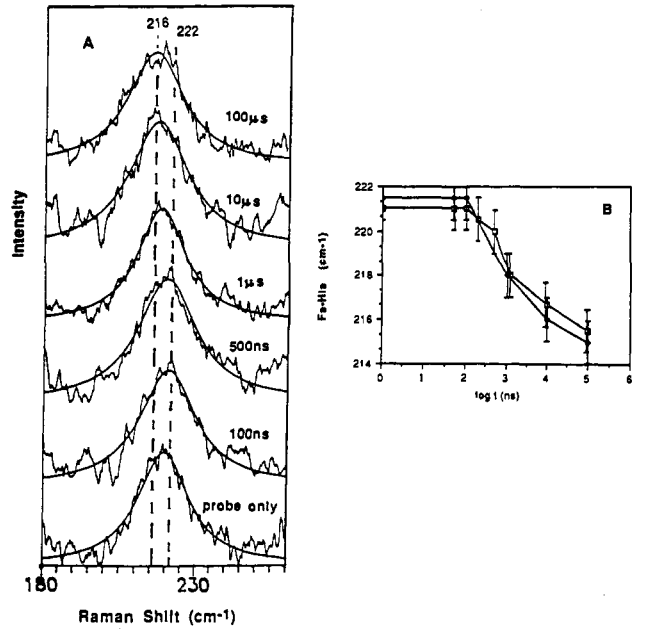

Figure 6. Panel A: Temporal evolution of the Fe–His mode in photolyzed MV–Cco enzyme. Panel B: Plot of Fe–His mode position vs log time subsequent to CO photolysis; (□) MV-Cco and (◆) FR-Cco. Spectra in panel A were analyzed as follows. The base line was adjusted using a linear two-point correction. The Fe–His band was then approximated as a single Lorentzian whose width, position, and intensity were allowed to vary independently. This procedure yielded acceptable fits ($\chi^2 < 0.25$) after fewer than 20 iterations in all cases. Using Gaussian line shapes did not affect the positions of the deconvoluted bands but did yield slightly larger line widths. The data points in panel B are the average of at least two sets of experimental data. Spectrometer accuracy was calibrated before and after each spectrum was acquired.

mental in elucidating the intermediates formed in the dioxygen reduction cycle of the enzyme.[26,27] Recently, however, it has become clear that the CO photodissociation *alone* is sufficient to produce complex structural dynamics at the ligand binding site.[18-21]

(26) Hill, B. C.; Greenwood, C. *Biochem. J.* **1984**, *218*, 913–921.
(27) Hill, B. C.; Greenwood, C. *Biochem. J.* **1983**, *215*, 659–667.

This study addresses two aspects of the structural dynamics of the cytochrome a_3 heme pocket. CO photodissociation triggers structural evolution of the protein environment associated with the heme–histidine bonding geometry (hereafter referred to as the proximal pocket, using the nomenclature of previous hemoglobin studies). It also initiates dynamics within that part of the heme pocket associated with exogeneous ligand binding (distal pocket). Our results indicate that protein conformational changes induced by the redox state of cytochrome a/Cu_A modulate only the latter of these processes.

Initial Response of the Cytochrome a_3 Heme Pocket to CO Photolysis. On the time scale of our studies (≥10 ns) CO photodissociation is an instantaneous event producing a high-spin, five-coordinate cytochrome a_3 complex. The extent of photodissociation can be regulated by changing the flux of the photolysis pulses and is reflected, at least qualitatively, in the relative intensities of ν_4 for the CO-bound (1368 cm^{-1}) and the unligated ferrous (1356 cm^{-1}) cytochrome a_3. The contribution of cytochrome a to this region of the spectrum varies with its redox state (ν_4(ferric) = 1372 cm^{-1}, ν_4(ferrous) = 1356 cm^{-1}) and thus complicates the quantification of the extent of CO photodissociation in studies of the MV enzyme.

High-flux laser pulses clearly generate a transient high-spin five-coordinate cytochrome a_3 which is distinct from the equilibrium species in both the FR and MV samples. These results are consistent with previous studies[17] which demonstrate that this photolytic transient species (1) exhibits a ν_{Fe-His} band which is higher in frequency by ~ 6 cm^{-1} than the equilibrium species and (2) can be generated using either B- or Q-band excitation of the heme a_3–CO complex. This behavior is similar to that exhibited by HbCO and presumably arises from an unrelaxed proximal heme pocket geometry. The initial transient configuration in photolyzed hemoglobins, however, varies with protein conformation (R/T) and solution conditions. In contrast, the FR and MV forms of Cco yield equivalent ν_{Fe-His} bands immediately after CO photodissociation under high-flux conditions. Thus, it appears that the transient proximal cytochrome a_3 geometry is not influenced by protein conformational changes predicted on the cytochrome a redox state.

The photodynamics of the cytochrome a_3–CO photolytic transient become more complex if low-flux photolysis pulses are used. Woodruff and co-workers[18,19] have recently performed a comprehensive series of studies which show that the early (<10 ns) dynamics of photodissociated cytochrome a_3–CO in FR-Cco are quite complex and involve the transient binding of CO to Cu_B. They also reported evidence for rapid binding (<1 ns) of an endogenous ligand (which presumably has been displaced from Cu_B subsequent to CO binding) to cytochrome a_3. This ligand (hereafter X) is apparently also photolabile. Thus under high-flux excitation it, too, is photodisociated by the pump pulses, producing the high-spin, five-coordinate cytochrome a_3 observed under those conditions. Spectra of photodissociated FR-Cco produced with low-flux excitation pulses do not show the distinct ν_{Fe-His} observed when high-flux pulses are used. Incomplete CO photodissociation would also be expected to reduce the intensity of ν_{Fe-His}, since this band is not observed for ligated cytochrome a_3–CO. Figure 1b–d indicates that the ν_{Fe-His} peak is absent over a range of photolysis levels of CO photodissociation (as evidenced by the corresponding spectra of ν_4). Interestingly, our attempts to generate the putative cytochrome a_3–X transient using lower flux Q-band excitation followed by low-flux ($\sim 2 \times 10^5$ W/(cm^2·s)) B-band resonance Raman scattering in a pump–probe protocol were also unsuccessful. At the higher photon fluxes produced by the 540-nm excitation, both cytochrome a_3–X and cytochrome a_3–CO are completely photolyzed.

The behavior of MV-Cco under low-flux conditions contrasts markedly to that observed for FR-Cco. Even under the lowest fluxes used, the relative intensity of ν_{Fe-His} of the photodissociated MV enzyme (measured against the intensity of either ν_4 at 1356 cm^{-1} or ν_8 at 340 cm^{-1}) remained nearly constant. Clearly, these observations reflect the differences in the distal heme pocket dynamics subsequent to CO photodissociation between the FR

and MV forms of Cco. The observed differences in the distal heme pocket dynamics most likely arise from structural variations in the distal pocket between the two forms of the enzyme. The following scenarios suggest themselves: (1) there is physical displacement of the ligand X away from the heme in MV-Cco, (2) there is an increase in the barrier for X-binding to the heme that slows down the kinetics in MV-Cco, or (3) the efficiency of heme a_3–X photolysis is significantly higher than that of heme a_3–CO photolysis. In view of the already high efficiency of CO photolysis, the last possibility is unlikely. We speculate that the first case is the most probable, since previous studies of the kinetics of exogeneous ligand binding[27] have suggested a more spacious distal heme pocket in MV-Cco.

Evolution of the Cytochrome a_3 Proximal Pocket Subsequent to CO Photolysis. The cytochrome a_3 conformation generated by CO photodissociation is a nonequilibrium species. It can evolve via ligand rebinding *or* structural relaxation to produce the equilibrium six- and five-coordinate cytochrome a_3 species, respectively. Previous studies[17-19] indicated that CO rebinding occurs on a much longer time scale than heme pocket structural relaxation. Unlike hemoglobins and myoglobins, there is little or no geminate heme–CO rebinding in photolyzed Cco–CO. Furthermore, the relaxation of the cytochrome a_3 proximal pocket (as monitored by the ν_{Fe-His} of the five-coordinate photolytic transient) is biphasic in the FR enzyme. It consists of a "lag phase" ($\sim$200 ns) in which no structural evolution is apparent in the Fe–His bond followed by a relaxation of ν_{Fe-His} ($\tau_{1/2}$ = 10 μs) from $\sim$222 cm^{-1} to its equilibrium position of $\sim$215 cm^{-1}. These previous studies were, however, conducted using high-flux probe pulses to generate time-resolved spectra. In view of the photolability of heme a_3–X, it is possible that these probe pulses may have influenced the results. The data obtained in this study trace the proximal pocket relaxation of both the FR and MV species under conditions where the probe pulse were too weak to initiate any photodynamics. Unfortunately, CO photolysis from the FR enzyme requires relatively high-flux (>3 × 10^6 W/(cm^2·s)) 540-nm pump pulses which yield only five-coordinate, high-spin heme a_3 photolytic transients (see above).

The conformational differences observed in MV-Cco, compared to FR-Cco, do not affect the temporal evolution of the heme a_3 proximal pocket. The Fe–His mode of heme a_3 evolves from 222 cm^{-1} to its equilibrium position (215 cm^{-1}) with $\tau_{1/2} \approx 10$ μs, following a 200-ns lag phase in which no relaxation takes place. As with FR-Cco, little or no ligand rebinding is observed on a 1-ms time scale.

Functional Implications of the Reduction of the Low-Potential Metal Centers in Cytochrome *c* Oxidase. The observed differences in transient behavior between FR-Cco and MV-Cco subsequent to CO photodissociation may be attributed to conformational differences at the cytochrome a_3–Cu_B site associated with the redox state of one or both of the low-potential metal centers. Previous studies by Dyer et al.[20] have demonstrated that, at room temperature, CO binds transiently to Cu_B^{1+} subsequent to photodissociation from cytochrome a_3 in FR-Cco. In addition, Woodruf et al.[18] have suggested that the binding of CO to Cu_B^{1+} triggers the release of a ligand from Cu_B^{1+} which transiently binds to cytochrome a_3. The data presented here indicates that such a "ligand shuttle" mechanism does not take place in the MV form of the enzyme. The lack of ligand binding to cytochrome a_3 subsequent to CO photodissociation indicates that here the conformation of the cytochrome a_3–Cu_B site is such that either the CO does not bind to Cu_B^{1+} or that, once CO is bound, the ligand displaced by CO does not bind to cytochrome a_3.

The apparent structural differences in the binuclear sites of FR-Cco and MV-Cco may be linked to the distinct electron-transfer pathways observed in recent time-resolved resonance Raman studies of the oxidation of both the FR and MV forms of Cco.[13-16] Room temperature time-resolved resonance Raman studies[13,14] of the early events in the oxidation of FR-Cco indicate that the initial electron transfer to bound dioxygen involves the rapid oxidation of the low-potential cytochrome *a* ($t_{1/2}$ = 3.5 × 10^4 s^{-1}), while in the MV form of the enzyme the initial electron transfer (from the high-potential Cu_B) occurs at a rate of 4.5 × 10^3 s^{-1}. It has previously been suggested, however, that the FR-Cco may represent a form of the enzyme that is not physiologically relevant.[28] The nonphysiological nature of FR-Cco is apparent, since under turnover conditions the population of FR-Cco is extremely small relative to that of other partially reduced forms of the enzyme. This scenario follows from the fact that the binding of dioxygen takes place extremely rapidly once both cytochrome a_3 and Cu_B become reduced.

The reduction of all four metal centers may have a profound effect on the electron-transfer pathways in cytochrome *c* oxidase placing the enzyme in a conformational state in which both pumping and nonpumping electron-transfer pathways are populated. Thus, the cytochrome a_3–Cu_B conformation in which the "ligand shuttle" mechanism is active (i.e., FR-Cco) most likely represents an uncoupling pathway that allows facile electron transfer from cytochrome *a* to the dioxygen reduction site.

Conclusions

The data presented here are consistent with previous observations of Woodruff and co-workers demonstrating that low-flux photodissociation yields a unique transient species in the FR enzyme that results from the rapid (<10 ps) binding of an endogeneous ligand, X, from the distal pocket of cytochrome a_3. The current study indicates, however, that there are possible conformational differences between the MV and FR forms of Cco that affect the distal pocket dynamics of cytochrome a_3. Specifically, the photolytic transient of MV-Cco yielded no evidence for heme a_3–X on the time scale examined in this study. We ascribe the conformational differences at the cytochrome a_3–Cu_B site between the FR and MV forms of the enzyme to reduction of one or both of the low-potential metal centers. Since the FR form of Cco may not represent a physiological conformation of the enzyme, it is unlikely that the putative heme a_3–X species plays a role in either the catalytic or proton-pumping functions of Cco.

(28) Larsen, R. W.; Pan, L. P.; Musser, S. M.; Li, Z.; Chan, S. I. *Proc. Natl. Acad. Sci. U.S.A.*, in press.